AN EXPERIMENTAL STUDY ON DRAG FORCE OF STONY DEBRIS FLOW

Takashi MATSUSHIMA[1], Kazumasa SATO[2], Yasuo YAMADA[3], and Senro KURAOKA[4]

[1]Member of ISSMGE, Associate Professor, Dept. of Engineering Mechanics and Energy, University of Tsukuba
(1-1-1, Tennodai, Tsukuba, Ibaraki 305-8573, Japan)
E-mail:tmatsu@kz.tsukuba.ac.jp
[2] Japan Railway Construction, Transport and Technology Agency
(6-50-1, Honmachi, Nakaku, Yokohama, Kanagawa 231-8315, Japan)
[3]Member of ISSMGE, Professor, Dept. of Engineering Mechanics and Energy, University of Tsukuba
(1-1-1, Tennodai, Tsukuba, Ibaraki 305-8573, Japan)
E-mail: yamada@kz.tsukuba.ac.jp
[4] Member of JSCE,, Nippon Koei Co., LTD
(2304, Inarihara, Tsukuba, Ibaraki 300-1259 Japan)
E-mail: a4982@n-koei.co.jp

In order to evaluate the drag force acting on Sabo facilities due to the impact of stony debris flow, small and large scale experiments were performed. Vertically-stacked cylindrical load cells were fixed at the downstream side to measure the drag force in dry granular flow or flow of gravel-water mixture. Flow velocity just before the impact was measured by PIV (Particle Image Velocimetry) technique. The measured force highly fluctuated with respect to time when the flow contained relatively large grains (boulders) compared to the sized of load cells. This fluctuation corresponds to impact force due to the collision of boulders, while the temporal average force is considered as the "equivalent" fluid force. The former is responsible for the failure of local members of the structure, while the latter is used for the design of overall structural stability. Experimental results show that the maximum impact force can be well described by the single collision model when the stiffness of the contact spring is correctly taken into account. On the other hand, it is found that not only the impact force but also the "equivalent" fluid force is affected by the particle size, which cannot be explained by a simple collision model or other fluid models.

Key Words : *Stony debris flow, drag force, particle size effect, collision model*

1. INTRODUCTION

Debris flow often causes tremendous disaster in mountain areas of intense precipitation. In order to design countermeasure facilities for the control of such debris torrents, it is necessary to evaluate their drag force acting on the structures. Debris flow is composed of various sizes of geological particles such as clay, sand, gravel and boulders mixed with water; the characteristics of such particles determine the overall properties of the flow. In the practical design, the material contents and the volume of the flow are estimated from the previous debris flow traces left at the target site, though it often includes much uncertainty. Even though the volume and the material contents of the debris flow are correctly evaluated, it is not easy to estimate the velocity of the flow and the drag force that includes the impact force of the relatively large geological particles and driftwood as well. In some design manual of Sabo facilities in Japan (eg., Sabo Technical Center 2001, National Institute for Land Infrastructure Management, 2007), the drag force due to debris flow is divided into two components: the temporal average force that is considered as the "equivalent" fluid force and the additional fluctuation regarded as impact force due to boulders and driftwood. The former is used for the overall structural stability design, while the latter is responsible for the local failure of the members of the structure.

In the aforementioned design manuals, the fluid force is estimated using the basic fluid mechanics which does not directly incorporate the effects of boulders. On the other hand, the estimation of impact force is based on a collision of a single boulder. In real stony-type debris flow, average grain size may affect the temporal average of drag force. Also, the effect of pore-water and so-called "multi-body interaction" between the boulders should be incorporated in the evaluation of the impact force.

This study focuses on this boulders' effect. A simple evaluation model based on the grain collision was applied to the estimation of both fluid force and impact force. Then a series of flow experiments with drag force measurement were performed for small scale dry granular flow and large scale grain-water mixture flow. The observed results are discussed together with the simple collision model to clarify the additional effects to be considered.

2. A SIMPLE COLLISION MODEL

We assume a spring-dashpot system at the contact between a solid particle and a structure. Then we begin with a very simple equation of motion of the particle:

$$m\ddot{u} + c\dot{u} + ku = 0 \tag{1}$$

where $u(t)$ is a contact depth, m is a mass of the particle, c and k are the constants of contact dashpot and spring, respectively. Solving this equation under the initial condition, $u(0) = 0$ and $\dot{u}(0) = v_0$, we obtain

$$u(t) = e^{-hnt}\frac{v_0}{n'}\sin n't \tag{2}$$

where $h = c/2\sqrt{km}$ is a damping coefficient, $n' = n\sqrt{1-h^2}$ and $n = \sqrt{k/m}$. Accordingly the impulse due to the collision is

$$S = \int_0^{T/2} ku\,dt = mv_0\{1 + \exp(-\frac{h}{\sqrt{1-h^2}}\pi)\} = mv_0(1+e_b) \tag{3}$$

where $T = 2\pi\sqrt{m/k}$ is a period of the oscillation and e_b is the restitution coefficient between the solid particle and the structure.

We assume that each collision occurs independently. The number of collision per unit time per unit area, N , is

$$N = \frac{M_S}{\rho_P V_P} = \frac{(1-\alpha)v_0}{V_P} \tag{4}$$

where M_S is a mass of particle portion hitting to the unit area of the structure per unit time (see **Figure 1**), ρ_P is a density of the particle solid, α is a porosity (volume of pore per unit volume) and V_P is the volume of a single particle.

Therefore the total impulse per unit time per unit area S_T is

$$S_T = S \cdot N = \rho_P(1-\alpha)(1+e_b)v_0^{\,2} \tag{5}$$

The bulk density of the flow ρ is described as

$$\rho = \begin{cases} \rho_P(1-\alpha) & \text{dry granular flow} \\ \rho_P(1-\alpha) + \rho_W\alpha & \text{grain water mixture flow} \end{cases} \tag{6}$$

Therefore, including the pore water effect, we have

$$S_T = \rho(1+e_b)v_0^{\,2} \tag{7}$$

Finally the equivalent fluid force per unit area $\bar{f}$ can be obtained as the temporal average of the drag force per unit area as follows:

$$\bar{f} = S_T \cdot 1 = \rho(1+e_b)v_0^{\,2} \tag{8}$$

This average is regarded as the "equivalent" fluid force. Comparing the quadratic drag (drag at high velocity) of a fluid per unit area

$$f_D = \frac{1}{2}C_D\rho v_0^{\,2} \tag{9}$$

we understand the drag coefficient $C_D = 2(1+e_b)$ in this simple model.

We may take another approach that consider the macroscopic momentum loss of the flow, then we have the similar equation:

$$f_M = (1-\frac{h_0}{h_1})\rho v_0^{\,2} \equiv \beta\rho v_0^{\,2} \tag{10}$$

where h_0 and h_1 are the flow height before and after the impact, and β is a rate of flow velocity reduction due to the structure. In the design of the slit-type Sabo dam, $\beta = 1$ is assumed for the safe side (Sabo

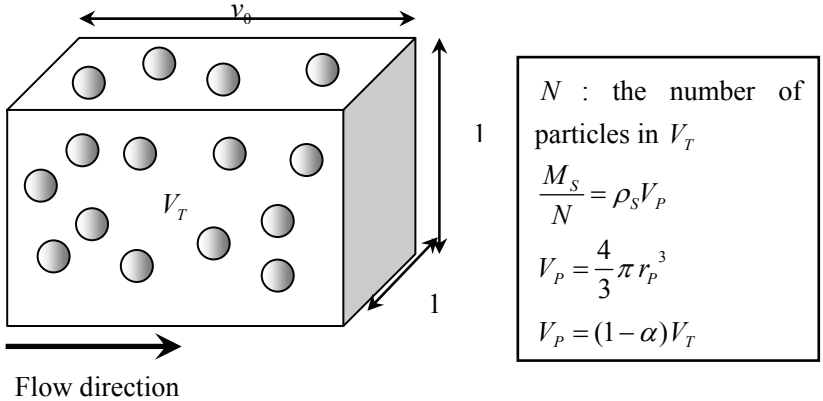

Figure 1 The volume of particle flow hitting to the unit area of the structure per unit time

Technical Center, 2001). According to the present simple collision model, however, β reaches 2 at maximum.

It should be noted that the equivalent fluid force $\bar{f}$ is independent of the particle size in this model. On the other hand, the fluctuation components of the drag force are dependent of particle size. When the flow particle is sufficiently small in comparison with the structure size, N is sufficiently large, and little fluctuation is observed. Accordingly, the additional impulse force becomes zero. On the other hand, when the particle size is relatively large compared with the structure size, the total impulse is not smeared and large fluctuation can be observed. The maximum force due to the collision of a single particle is simply described as follows:

$$f_{\max} = \sqrt{mk}\, v_0 \tag{11}$$

3. EXPERIMENTS OF SMALL-SCALE DRY GRANULAR FLOW

In order to investigate the effect of boulder impact force, a series of simple experiments on dry granular flow was performed. **Figure 2** shows the experimental setup. A waterway of 150 cm long, 15.4 cm wide was designed so as to take at an arbitrary angle and granular material was stored in a hopper at the upstream end. The floor of the waterway was made of a smooth acrylic plate. Stacked cylindrical load cells of about 38 mm diameter (**Figure 3**) were fixed at the waterway (80 cm downstream from the hopper) to measure the drag force of the granular flow at different heights. Materials used in the experiments are listed in **Table 1**. Glass beads A and B have quite spherical shape, while Toyoura sand particles have irregular shape (sub-angular in usual soil mechanics classification). The granular flow was monitored by a high speed camera from the side or above, so that the obtained images could be analyzed with PIV (Particle Image Velocimetry) technique to detect the velocity of the flow just before impacting the load cells. In order to get the clear particle image suitable for PIV, transparent glass bead particles were colored. The height of the flow was also captured from the images taken by the side camera.

A series of experiments was performed with different slope inclinations. **Table 2** shows the summary of the experiments. The height of the flow, H, the velocity of the flow, V, the forces obtained by the load cells at different flow heights (0 to 1 cm, 1 to 2 cm, 2 to 3 cm) in the table are the maximum values observed around $t = 0.5$ (sec).

Figure 4 shows an example of the results of PIV analysis (Toyoura sand, slope angle=35 deg.) where almost homogeneous velocity field is obtained. The average velocity computed by such PIV analysis is plotted with respect to time in **Figure 5**. The height of the flow in time sequence is plotted in **Figure 6**.

Table 1 Materials used in the experiments

	Relative density	Max. grain size (mm)	Min. grain size (mm)	Ave. grain size (mm)
Glass beads A	2.5	0.25	0.18	0.215
Glass beads B	2.5	3.35	4.75	4.05
Toyoura sand	2.64	about 0.4	about 0.1	0.206

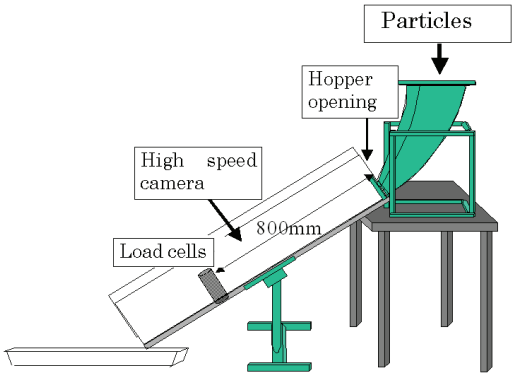

Figure 2 Experimental setup of small-scale dry granular flow

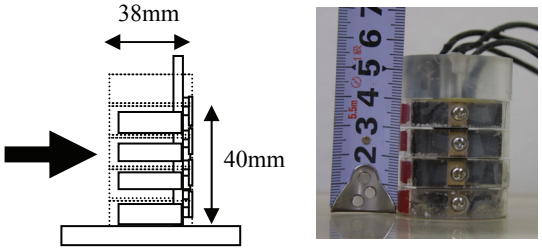

Figure 3 Stacked load cells

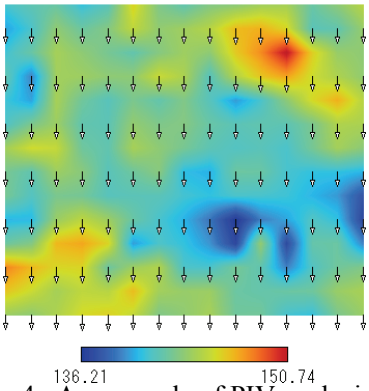

Figure 4 An example of PIV analysis (top view)

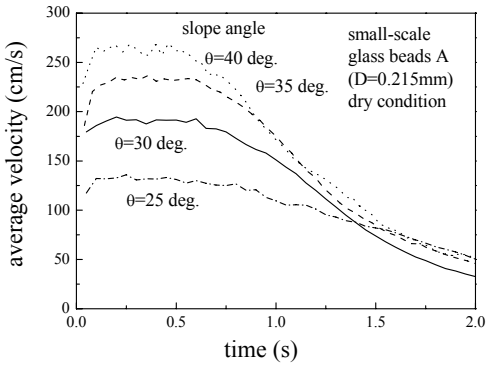

Figure 5 Average velocity obtained by PIV analysis with respect to time

Table 2 Summary of experiments

Small-scale	θ (deg)	H (cm)	V (cm/s)	F (0-1)	F (1-2)	F (2-3)	F_{total} (N)	$F_{total}/(3H_{LC}D_{LC})$ (kPa)
Toyo(D0.2)	30	1.7	60	0.12	0.08	0.01	0.21	0.55
	35	1.25	130	0.25	0.25	0.1	0.6	1.58
	40	1.2	200	0.43	0.30	0.15	0.88	2.32
Glass beads A (D0.215)	25	1.6	130	0.25	0.23	0.15	0.63	1.66
	30	1.6	190	0.43	0.43	0.23	1.09	2.87
	35	1.65	230	0.58	0.59	0.3	1.47	3.87
	40	1.7	260	0.73	0.75	0.35	1.83	4.82
Glass beads B (D4.05)	25	1.35	180	0.8	0.55	0.25	1.6	4.21
	30	1.4	220	0.95	0.7	0.35	2.0	5.26
	35	1.35	265	1.6	1.1	0.4	3.1	8.16
Large-scale				F (0-4)	F (4-8)	F (8-12)	F_{total} (N)	$F_{total}/(2H_{LC}D_{LC})$ (kPa)
Case 1		8	400	9.0	8.5	0	17.5	0.547
Case 2		8	200	3.0	1.0	0	4.0	0.125
Case 3		8	290	3.0	4.5	0	7.5	0.234
Case 4		8	290	5.0	5.0	0	10.0	0.313
Case 5		8	290	8.0	5.0	0	13.0	0.406
Case 6		8	290	10.0	6.0	0	16.0	0.5

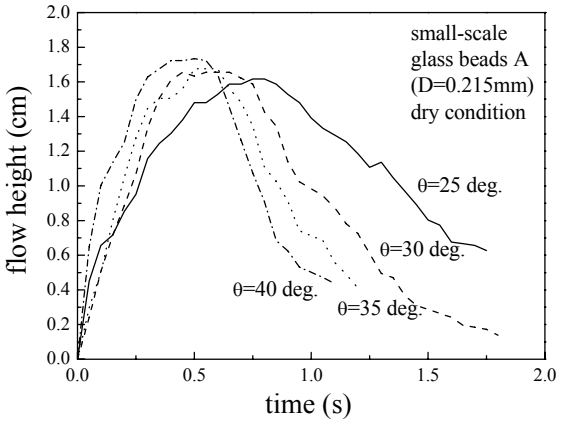

Figure 6 An example of time history of flow height

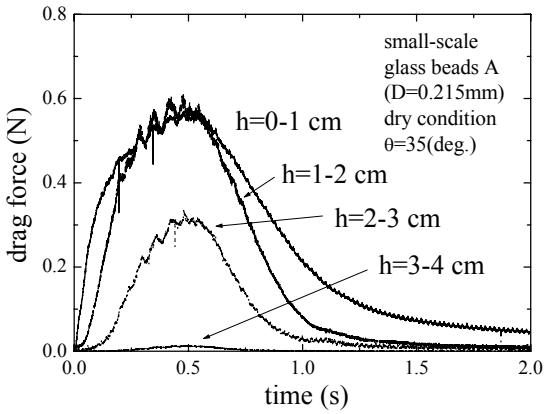

Figure 7 Drag force measured by the stacked load cells (Grass beads B (D=0.215mm))

Figure 7 shows the drag force, F, measured by the stacked load cells. Since the particle size of glass beads A ($D = 0.215$ mm) is small enough in comparison with the diameter of the load cells (D_{LC} =38mm), the observed curves are sufficiently smooth and the fluctuation is not predominant. The same tendency was also observed in the case of Toyoura sand whose diameter was about 0.20mm though the drag force itself was rather smaller. It is because the flow velocity was relatively small affected by its irregular particle shape. The relation between the flow velocity and the drag force is discussed subsequently. On the other hand, the observed drag force shows noticeable fluctuation in the case of glass beads B ($D = 4.05$ mm) (**Figure 8**), whose particle diameter is about 1/10 of the size of the load cells. The figure also shows its temporal average (average of the closest 500 data), $\overline{F}$. $\overline{F}$ divided by the effective area of the load cell, $D_{LC} \cdot H_{LC}$, its diameter multiplied by its height, may correspond to $\bar{f}$ in equation (8).

4. EXPERIMENTS OF LARGE-SCALE GRAVEL-WATER MIXTURE

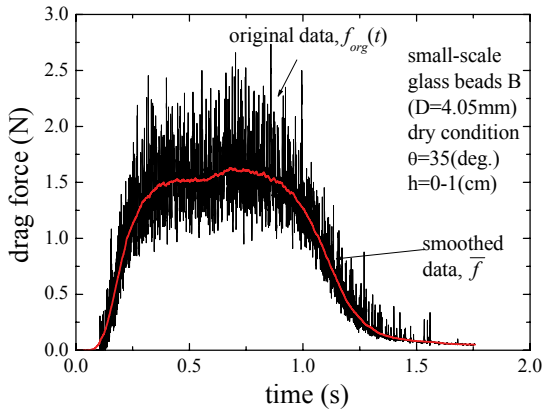

Figure 8 Drag force for the flow of Grass beads B (D=4.05mm)

The similar experiments described above were performed with large-scale waterway of 10 m long

and 50 cm wide. Gravels whose diameter ranged from 9.0 mm to 30 mm were sieved into two sizes (9.0 mm to 19.5 mm and 19.5 mm to 30 mm) and then mixed with different fraction to investigate the effect of gravel size. Then the gravels were streamed with different volume of water. **Table 3** summarizes the experimental conditions.

Similarly to the case of small-scale experiments, a set of load cells of D_{LC} =40mm in diameter and a high-speed camera were installed to measure the drag force and flow velocity, respectively.

Figure 9 shows the time history of the flow velocity of the mixture just before hitting to the load cells. The inclination of the slope and the location of the load cells are identical in all the cases. The flow velocity in case 1 was much bigger than that in case 2 because of the water contents. The flow velocities in cases 3 to 6 were almost identical even with the different mean particle size (The volume fraction of gravel to water was identical.)

Figure 10 is an example of the drag force measured by the load cell. The observed large fluctuation was due to the collision of gravels. The temporal average of the drag force around t=0.5 to 1.0 (s) for all the cases are summarized in **Table 2**.

5. DISCUSSION

Figure 11 shows the relationship between the square of the flow velocity multiplied by the bulk density of the flow, ρ, and the temporal average of the drag force $\overline{F}$ divided by the effective area of the load cell ($D_{LC} \cdot H_{LC}$, its diameter multiplied by its height) for all the experiments described above. The bulk density in large-scale experiments on gravel-water mixture flow was simply calculated from their volume contents and roughly-estimated gravel density ρ_P =2.5(g/cm^3). As for the small-scale dry granular flow, ρ was calculated from the information on the time history of the height and the velocity of the flow, which was around 1.0(g/cm^3) for all the cases.

Even in the wide variety of materials as well as flow conditions, the results shown in **Figure 11** lie within a limited area, which is characterized by the linear relation with its inclination between 0.25 and 1.2. According to equation (7), the inclination is described by $(1+e_b)$ that basically ranges from 1 to 2. The inclination obtained by the experiments is lower than this range, primarily because of the multi-body effect; the rebounding particles collide with other particles, which may reduce the colliding velocity and accordingly reduce the effective damping coefficient. Pore water may also reduce the effective damping coefficient to some extent.

Another important issue is that the particle size effect is clearly seen both in small-scale dry granular flow and large-scale flow of gravel-water mixture. In the latter case, the temporal average drag force increases almost linearly with increasing gravel size. Since the above mentioned drag force evaluation model does not include this effect, it is necessary to take it into account.

When the impulse components of the drag force observed in relatively large particles is concerned, the simple collision model gives a reasonable estimation. **Figure 12** shows the close-up of the drag force time history for case 1 of the large-scale experiments. According to this figure, the vibration has some predominant period. The result of Fourier

Table 3 Experimental conditions

	Volume of gravels (19.5 to 30.0 mm) (cm^3)	Volume of gravels (9.0 to 19.5 mm) (cm^3)	Volume of water (cm^3)	Average density ρ (g/cm^3)
Case 1	0	31200	516000	1.09
Case 2	0	31200	129000	1.29
Case 3	0	62400	333000	1.24
Case 4	20800	41600	333000	1.24
Case 5	41600	20800	333000	1.24
Case 6	62400	0	333000	1.24

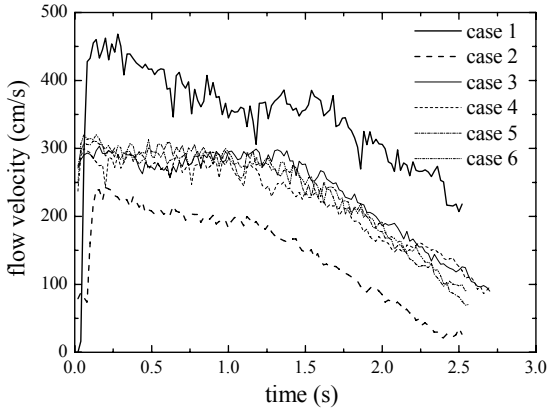

Figure 9 Flow velocity for large-scale experiment on gravel-water mixture flow

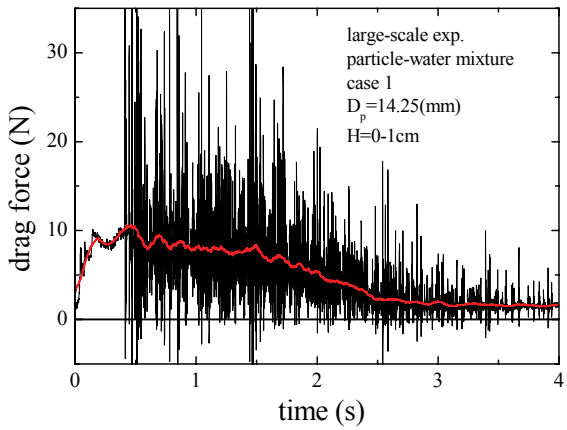

Figure 10 An example of drag force measured by load cells

analysis of this vibration is shown in **Figure 13**, which indicates the predominant frequency λ is about 380 Hz. Using the elementary equation

$$\lambda = \frac{1}{2\pi}\sqrt{\frac{k}{m}} \qquad (12)$$

and the mass calculation of a single particle, we obtain the spring coefficient k=22000(kg/s^2). Since this value is much smaller than that of gravels evaluated by Hertz contact theory (Johnson 1982), it must be due to the stiffness of the load cell. Putting this value into equation (11), we can compute the maximum force of a single collision, f_{max}=36(N), which is in good agreement with the observed impulse force shown in **Figure 12**. The good agreement is also found in other cases including the dry granular flow.

6. CONCLUSION

In order to clarify the effect of particle size on the drag force acting on the Sabo facilities due to stony debris flow, experiments on small-scale dry granular flow and large-scale gravel-water mixture flow were conducted. When the particle size was not negligible compared with the size of load cells, the observed drag force was drastically fluctuated. The temporal average of the drag force was affected by the particle size. It is necessary to put this effect into the drag force evaluation models. Maximum impact force due to the collision of gravels can be well described by the single collision model when the stiffness of the contact spring is correctly taken into account. Further study is needed on the effect of density and depth of the flow, grain size distribution and others.

ACKNOWLEDGMENT: This research was partially supported by the Ministry of Education, Science, Sports and Culture, Grant-in-Aid for Scientific Research (B), No. 18360223, 2006-2009.

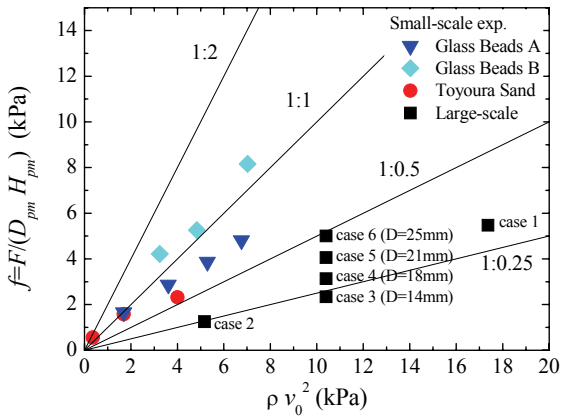

Figure 11 Relationship between the "equivalent" fluid force and ρv_0^2

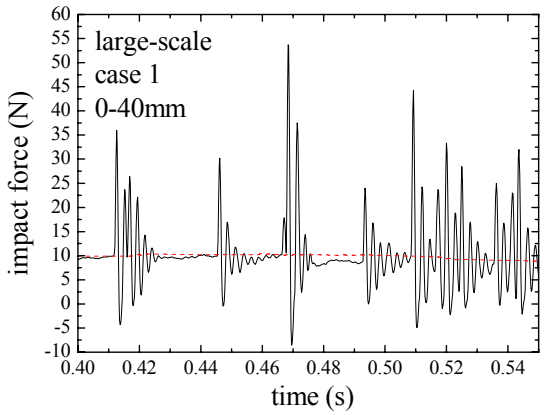

Figure 12 An example of impact force (close-up of Figure 10)

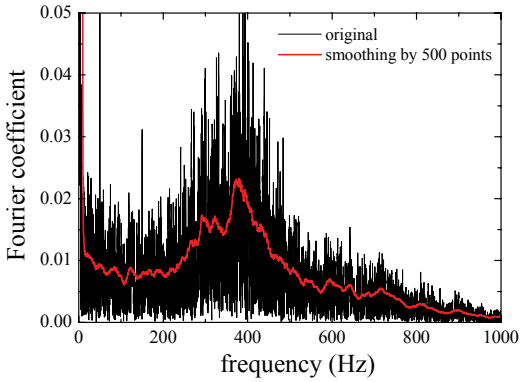

Figure 13 Fourier analysis result for the drag force in case 1

REFERENCES

1) Sabo Technical Center: Design Manual for Steel Open-type Sabo Facilities, 2001 (in Japanese).
2) National Institute for Land Infrastructure Management: Manual of Technical Standard for designing Sabo facilities against debris flow and driftwood, Technical note of NILIM, No. 365, 2007 (in Japanese).
3) Iverson, R.M.: The physics of Debris Flows, Reviews of Geophysics, 35, 3, pp. 245-296, 1997.
4) Takahashi, T.: Debris flow, IAHR, Monograph series, Balkema, 1991.
5) Matsushima, T., Kameda, T., Sato, K.: A Debris-Flow Countermeasure suitable for Robotized Construction, Proc. 10th Symposium on Automation and Robotics in Construction, pp.163-172, 2004 (in Japanese).
6) Sato, K.: Effect of particle characteristics on drag force of debris flow, Master Thesis, Graduate School of Systems, and Information Engineering, University of Tsukuba, 2006 (in Japanese).
7) Johnson, K.L., Contact mechanics, Cambridge University Press, 1985.